Research Report

Measurement and Estimation Technologies for the Experimental Analysis of Metal V-belt Type CVTs

Hiroyuki Yamaguchi, Hirofumi Tani, Kisaburo Hayakawa

Abstract

This paper outlines measurement and estimation technologies necessary for solving metal V-belt CVT issues. These technologies examine the detailed behavior of the working belt. The test apparatus consists of a low inertia dynamo with high response that can reproduce the transitional characteristic similar to engines. To analyze power transmission characteristics, we construct a measurement technology that clarifies the transitional characteristic and transmission performance around the marginal torque of the belt. In addition, we construct estimation technologies as a substitute for the measurements of working belt behavior, which is difficult to measure in an actual system. In this paper, we discuss cases of a special experimental technology for metal V-belt type CVTs.

Keywords CVT, Metal V-belt, Friction characteristic, Working state, Measurement, Observer, Low inertia dynamo

1. Introduction

The metal V-belt CVT has gained popularity as a means of reducing fuel costs. Issues confronting CVTs is to approach an ideal power transmission mechanism through improvements in transfer efficiency, torque capacity, durability, and quietness that would make the CVT superior to conventional AT. Solutions to these issues require the analysis of the power transmission characteristics of the belt, and various belt behavior measurements have already been examined. However, as the understanding of working belt behavior advances, a more detailed analysis of working belt behavior is needed.

In response to this need, this paper presents a new test apparatus and new technologies for measuring and estimating belt behavior. We first discuss the low inertia dynamo with high response, which can reproduce the transitional characteristics similar to engines. Next, with regard to the analysis of torque transmission mechanism, we discuss a method for measuring element strain that uses sensing parts to detect load and minute behavior. We then discuss a method for measuring the pitch radius of a pulley. This method, which measures the pitch radius even during changes in the speed ratio, is needed for the measurement of the friction characteristic between the pulley and the belt. We also discuss estimation technologies for belt velocity and the marginal performance of transmission torque. These technologies are necessary to examine the belt marginal performance, which is difficult to measure in actual systems.

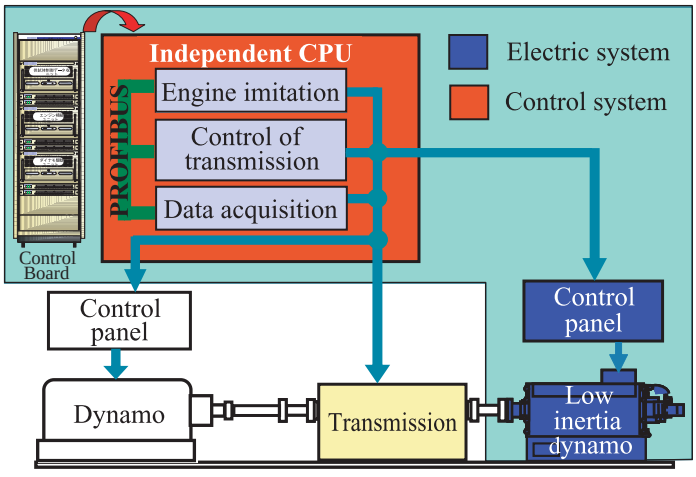

Fig. 1 Dynamo control system.

2. Driving apparatus (low inertia dynamo)

A low inertia dynamo that can reproduce an engine was used to research a static maximum friction coefficient and a dynamic friction coefficient for the input torque and belt slip velocity in a CVT.[1, 2] **Table 1** shows the specification. The moment of inertia of the dynamo is appropriate for a mid-level engine. As shown in **Fig. 1**, the low inertia dynamo system consists of a control board that drives the dynamo, which is connected to both ends of the transmission, and a control system for inputting commands to the control board. The control system easily reproduces the driving conditions of engines because it is configured from the general-purpose control system design software Matlab/Simulink. Because the dynamo torque control is feed-forward of the command current through high-speed digital communication, the maximum response frequency of the torque is 500 Hz, as shown in **Fig. 2**. Moreover, the speed response of the low inertia dynamo surpasses that of conventional dynamos to an extent that allows it to follow changes in the target rotating speed of about 8000 rpm at around 10 Hz and of 1000 rpm below 1 Hz, as shown in **Fig. 3**.

The following describes examinations of the CVT that take advantage of the high response of the low inertia dynamo. As shown in **Fig. 4**, the test apparatus cordons off space for the pulley, the belt, and the box, and facilitates the installation of

Table 1 Specification of low inertia dynamo.

Type	Three-phase induction motor
Output power	220kW
Moment of inertia	0.098kgm^2
Rated speed	6000rpm
Max speed	8000rpm
Allowable torque	350Nm (Constant@6000rpm)
	550Nm (60 seconds@6000rpm)

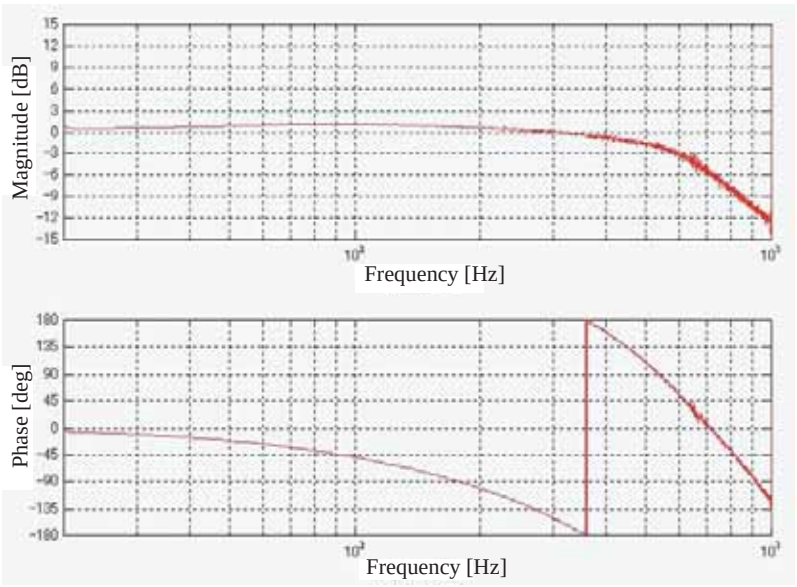

Fig. 2 Torque response of low inertia dynamo.

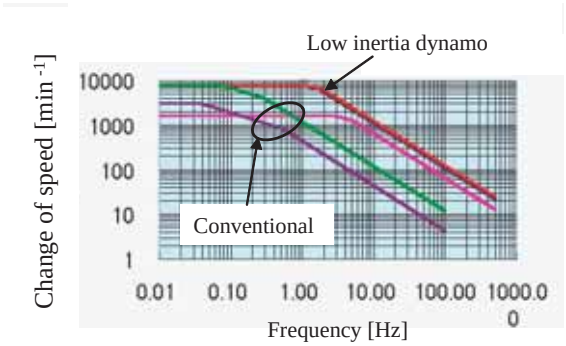

Fig. 3 Speed response of low inertia dynamo.

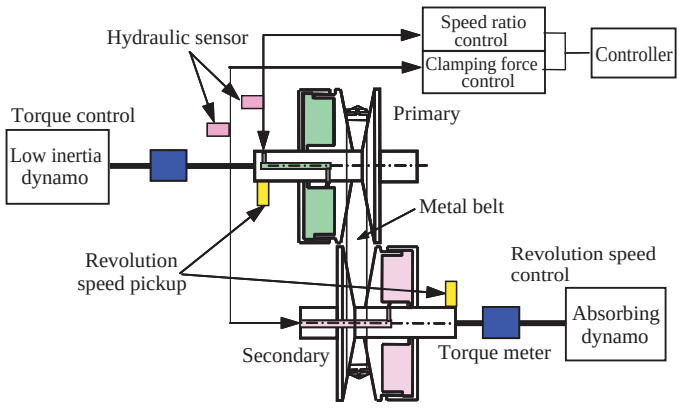

Fig. 4 Schematic of test apparatus.

sensors. A primary pulley and a secondary pulley are connected to the low inertia dynamo and to an absorbing dynamo, respectively. The former is controlled by torque, the latter by revolution speed. Both pulleys are made movable by controlling oil pressure. The transmitting torque and the speed ratio are controlled by servo valves. An example of measuring the maximum friction coefficient of the belt is shown in **Fig. 5**. Input torque is increased gradually while keeping the speed ratio and the clamping force of the secondary pulley constant. The beginning of a macro slip (large belt slip) is detected when the slip ratio suddenly increases. Shortly thereafter, the input torque can be rapidly decreased to prevent persistence of the macro slip. The relation between a macro slip and the input torque near the belt slip limit is shown in Fig. 5. While the amplitude of input torque vibration is gradually increased at a constant speed ratio, input torque, and speed ratio, the input torque suddenly changes near the black line in Fig. 5 and macro slip occurs. From this point, it is possible to find a slip limit for the input torque. It can be expected that the friction characteristic, the transmission efficiency characteristic, and the stress characteristic under

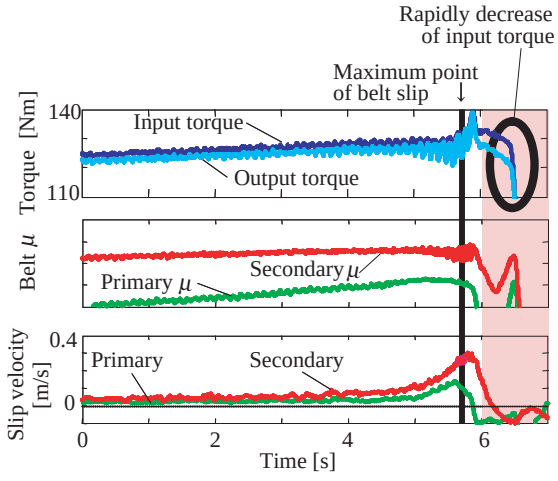

Fig. 5 Friction coefficient at a belt slip limit.

dynamic behavior, which hitherto have not been clearly understood (for example, changes in input torque and in speed), will be clarified.

3. Measurement technology

3. 1 Belt element strain measurement

With an understanding of the load that acts on the each element part during one belt rotation cycle, the measurement of belt element strain is an effective means for analyzing the torque transmission mechanism and for estimating element strength. In addition, it is possible to use strain to examine minute movements (for instance, interference in the nose during element alignment and posture change in the pulley) by examining strain of the measurement part.

The usual methods for measuring strain in a rotating body are wired measurement using a slip ring and wireless measurement using a telemeter. For the following reasons, we used the new data-logger system[3)] to measure element strain. First, the effect on object behavior is small, and high-speed measurements can be made because the system is wireless and light (approximately 5g). Second, installation of a slip ring or an antenna is not required, and measurements can be made as necessary in actual transmissions.

The measurement system employing a strain sensor and the data-logger system is shown in **Fig. 6**. The strain sensor has a slit around the nose of the element to enable measurement of the load acting on the nose. As an example, **Fig. 7** shows the results of a measurement at deceleration. In the string of compression area in this figure, the compression load characteristic of the push type belt is confirmed. Also in this figure, interference in the nose is confirmed at the starting point and the terminal on the string of slack area. **Figure 8** shows the strain sensor in which gauges are placed on the right and left and on the inside and outside to measure compression and bending that act on the direction of the element width. The result of the acceleration measurement is shown in **Fig. 9**. A large clamping force can be presumed in the vicinity of the pulley

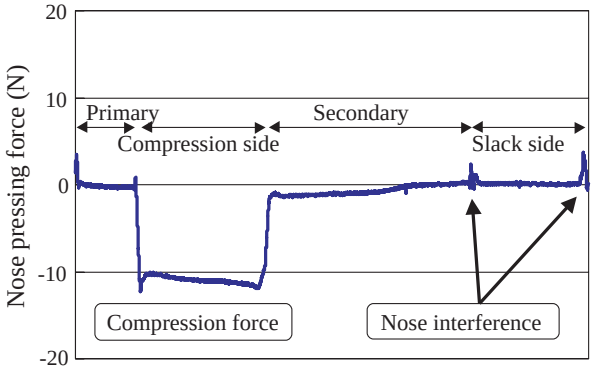

Fig. 7 Measurement result of element nose strain. (N_{in}=500rpm, T_{in}=150Nm, speed ratio=2.4)

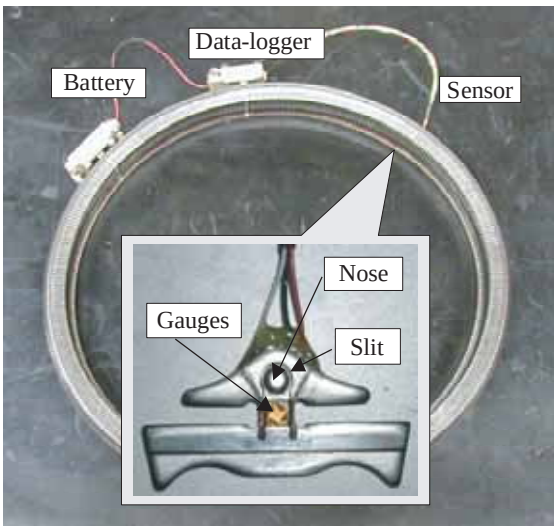

Fig. 6 Nose load sensor and data-logger system.

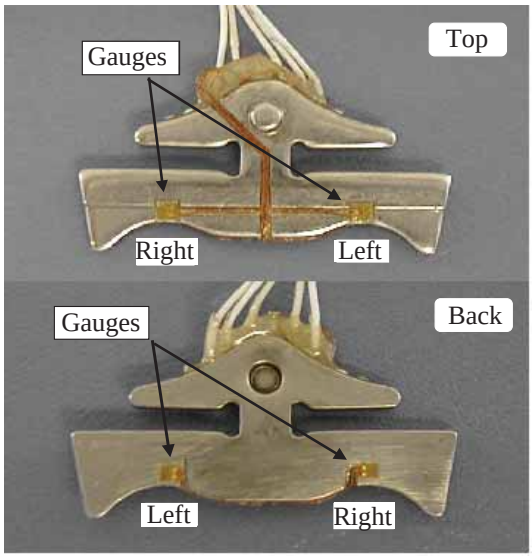

Fig. 8 Width direction load sensor.

exit from the compression strain. Also, a rightward element yaw can be presumed in the secondary pulley from the right as well as leftward bending strain.

3. 2 Pitch radius measurement

Because the belt slip velocity is necessary for the measurement of belt friction coefficient and transfer loss, the pitch radius must be measured.

Pitch radius is usually measured with gap sensors fixed to the housing. For the following reasons, we use direct measurement employing a long-stroke (50 mm) linear gauge attached to a hard alloy chip in the tip.[2] First, there is little sensor damage because a hard alloy chip is used for the belt contact part. Second, the pitch radius can be measured at any speed ratio from deceleration to acceleration without rearrangement of the measurement system. Third, even if the amount of element head clearance changes in response to the speed ratio, the measurement results are not affected. Although this method is not suitable for high-speed measurement because of the contact type, measurement up to about 1500 rpm is possible.

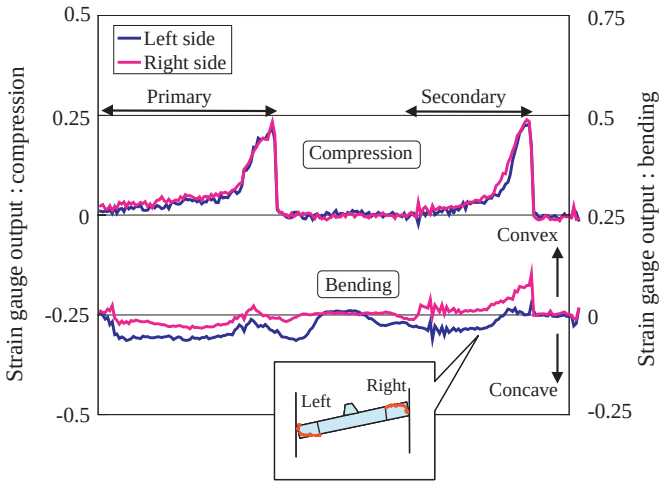

Fig. 9 Measurement result of element width direction strain. (N_{in}=1000rpm, without load, speed ratio=0.7)

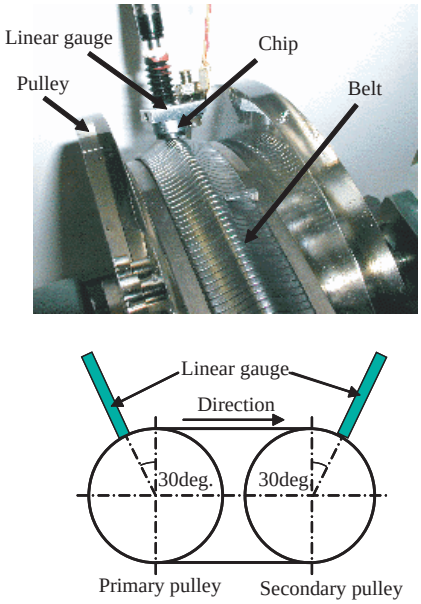

Fig. 10 Pitch radius measurement device.

The pitch radius measurement device is shown in **Fig. 10**. An example of measuring the pitch radius of the primary and secondary pulleys when the speed ratio is controlled is shown in **Fig. 11**. We found that the primary pitch radius becomes large and the secondary pitch radius becomes small when the torque is increased. This finding confirms that the speed ratio is kept constant by the pitch radius ratio of the pulleys being controlled on the acceleration side, since the belt slip increases with an increase in torque.

3. 3 Measurement of the friction characteristic between the pulley and the belt

Reducing the belt clamping force is effective for improving the efficiency of the CVT. However, extreme reduction causes macro slip. Before an adequate clamping force can be set, the friction

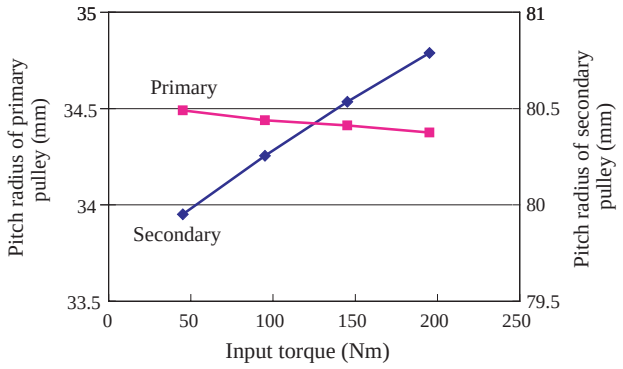

Fig. 11 Measurement result of pitch radius. (N_{in}=1000rpm, speed ratio=2.4)

characteristic between the pulley and the belt and the torque margin of the belt must be understood. In addition, the belt is subject to being overpowered by disturbance torque such as engine cyclic torque fluctuations or by tire torque on an uneven road. Accordingly, the effects of the disturbance torque on the friction characteristic must also be understood. The following describes the characteristic of the belt friction coefficient (referred to hereafter as belt μ) according to the static input torque and the torque fluctuations.

Belt μ and slip velocity between the pulley and the belt are calculated as follows:

$$\text{Belt } \mu = T \cdot \cos(\theta) / (2 \cdot R \cdot F) \quad \cdots\cdots\cdots\cdots\cdots (1)$$

Slip velocity of primary:

$$\Delta V_p = R_p \cdot \omega_p - V \quad \cdots\cdots\cdots\cdots\cdots (2)$$

Slip velocity of secondary:

$$\Delta V_s = V - R_s \cdot \omega_s \quad \cdots\cdots\cdots\cdots\cdots (3)$$

where the following variables are used:

T : Given torque for pulley [Nm]
θ : Flank angle of pulley [deg]
2 : Number of pulley faces contacting belt
R : Pitch radius of pulley [m]
F : Clamping force of pulley [N]
ω : Revolution speed of pulley [rad/s]
V : Belt velocity [m/s]

The suffixes p and s indicate primary and secondary.

In Eqs. (1) to (3), torque is measured by a torque meter, rotation speed is measured by revolution pick-up, and the radius pitch of belt is measured using the method described earlier. The clamping force is obtained from compensation of the centrifugal hydraulic pressure for the measured value from the hydraulic pressure sensor. Belt velocity is obtained from measurement of the belt cyclic time using the response of a gap sensor on a metal chip attached to the ear part of a belt element. The result of measuring static belt μ (slip side pulley) is shown in **Fig. 12**. This result is obtained by increasing the input torque while keeping the speed ratio and secondary clamping force constant. The relation between slip velocity and belt μ for each speed ratio is shown in **Fig. 13**. As shown in the figure, the slip velocity becomes large and the belt μ_{max} becomes small at γ = 2.30 (high speed ratio).

A method for investigating belt slip by input torque fluctuations is shown in **Fig. 14**. The amplitude of the vibration torque gradually increases until macro slip occurs. The secondary clamping force is set just enough for average torque. The experimental parameter is vibration frequency. The ratio of the vibration amplitude to the average torque when macro slip occurs is shown in **Fig. 15**. The torque margin for macro slip becomes large as the frequency and the revolution speed become high.

4. Estimation technology

The motions of the working belt should be investigated not only in the CVT but also in a vehicle. However, it is difficult to put a vehicle on the sensors described above. This

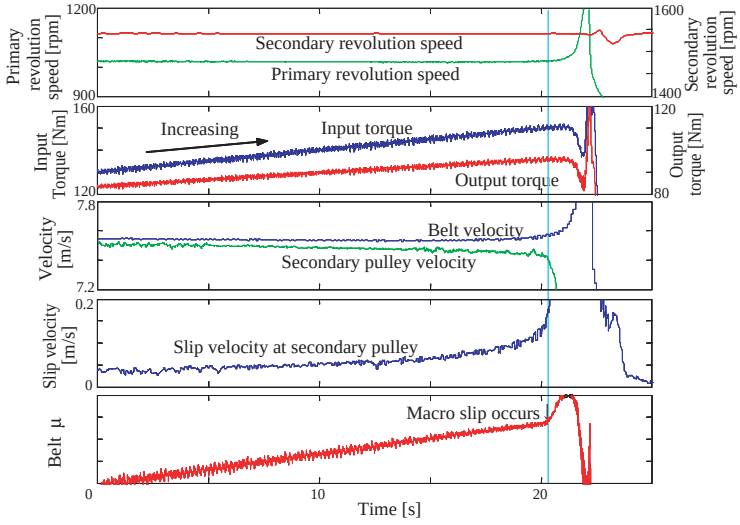

Fig. 12 Measurement result of static belt μ.
(speed ratio=0.65, N_{in}=1000rpm)

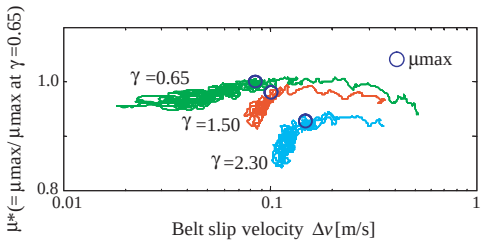

Fig. 13 Relation between slip velocity and belt μ.
(N_{in} =1000rpm, T_{in} =100Nm)

section describes estimation methods that can be substituted for measurements. There are two methods: one for estimating belt velocity in the calculation of belt slip velocity and the other for estimating the friction margin of the belt in the analysis of the friction characteristic.

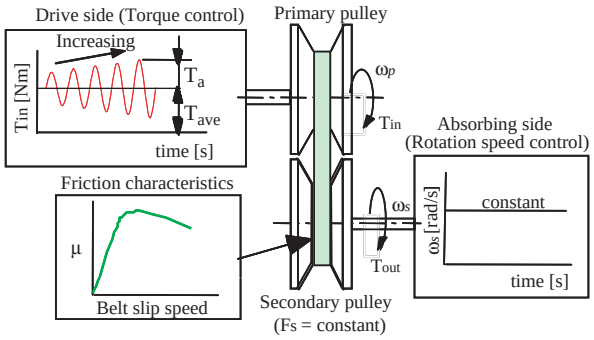

Fig. 14 Method to investigate belt slip by input torque fluctuations.

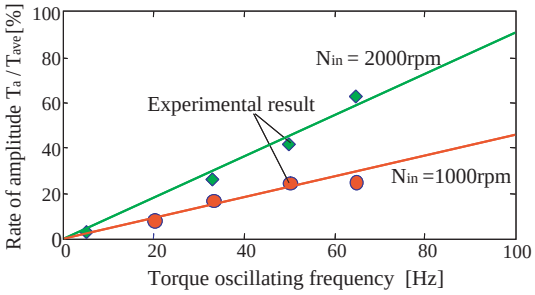

Fig. 15 Ratio of vibration amplitude to the average torque at macro slip occurrence. (T_{ave} = 100Nm, speed ratio = 0.65)

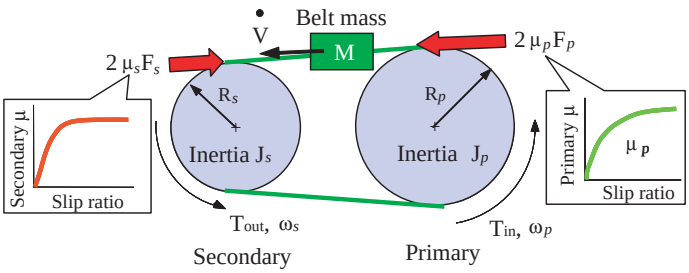

Fig. 16 Model based on belt velocity estimation.

4. 1 Sensors used

The sensors used to make the estimations are hydraulic pressure sensors and revolution speed sensors. The input torque signal is estimated using the throttle opening, vehicle speed, and air-fuel ratio instead of torque sensing. The estimated torque has an approximate error of 10%. The output torque signal is obtained as the product of the estimated torque and the speed ratio. The pitch radius of the pulleys are determined by the center distance, belt length, and speed ratio.

4. 2 Estimation of belt velocity

The belt velocity is estimated by using a physical model that describes the balance between belt friction forces and torque (**Fig. 16**). The belt mass is driven by the difference of the friction force between the two pulleys. The motion is expressed as follows:

$$J_p \cdot \dot{\omega}_p = -2 \cdot \tilde{\mu}_p \cdot F_p \cdot R_p + \hat{T}_{in} \cdot \cos(11^\circ) \quad \cdots\cdots (4)$$

$$J_s \cdot \dot{\omega}_s = 2 \cdot \tilde{\mu}_s \cdot F_s \cdot R_s - \hat{T}_{out} \cdot \cos(11^\circ) \quad \cdots\cdots (5)$$

$$M \cdot \ddot{\tilde{V}} = 2 \cdot \tilde{\mu}_p \cdot F_p - 2 \cdot \tilde{\mu}_s \cdot F_s \quad \cdots\cdots (6)$$

In the equations, the symbols ~ and ∧ indicate unknown parameters and estimated values, respectively. The differential term of the belt velocity is included on the left side of Eq. (6). Equations (4) to (6) are the basic equations for the estimation. By reducing the number of unknown parameters the accuracy of the estimation can be improved. The friction characteristic is used as an approximated characteristic in the following equation:

$$\mu_p = \mu_{p\max} \cdot (1 - \exp(-\alpha_p \cdot \tilde{slip}_p)) \quad \cdots\cdots (7)$$

Here,

$$\tilde{slip}_p = (\omega_p \cdot R_p - \tilde{V}) / (\omega_p \cdot R_p) \quad \cdots\cdots (8)$$

Although Eqs. (7) and (8) apply to the primary pulley, they are the same for the secondary pulley. The result of the approximation using Eq. (7) is shown in **Fig. 17**, and nearly coincides with the true characteristic of belt μ shown in Fig. 17. Equations (4) to (6) schematically express the motion between the belt and the pulleys, and Eqs. (7) and (8) include

an approximation error of the belt μ characteristic. The result of the belt velocity estimation has a large error due to integration of the belt acceleration based on Eqs. (4) to (8). The estimation error should be eliminated by calibrating the belt velocity by constructing a state observer,[4] but it is difficult to construct the observer because Eqs. (7) and (8) have nonlinear parameters. Equation (7) is linearized as follows:

$$\mu_p = \partial\mu_p / \partial \mathrm{slip}_p \cdot \tilde{\mathrm{slip}}_p + \mu_{p0}$$
$$= \mu_{pg} \cdot (\omega_p \cdot R_p - \tilde{V}) + \mu_{p0} \quad \cdots\cdots\cdots (9)$$

Here,

$$\mu_{pg} = (\partial\mu_p / \partial \mathrm{slip}_p) / (\omega_p \cdot R_p) \quad \cdots\cdots\cdots (10)$$

$$\mu_{p0} = \mu_p - \mu_{pg} \cdot (\omega_p \cdot R_p - \tilde{V}) \quad \cdots\cdots\cdots (11)$$

The observer is constructed based on Eqs. (4) to (6) and Eqs. (9) to (11).

$$\dot{\hat{\mathbf{X}}} = \mathbf{A} \cdot \hat{\mathbf{X}} + \mathbf{B} \cdot \mathbf{U} + \mathbf{K} \cdot (\mathbf{Y} - \hat{\mathbf{Y}}) \quad \cdots\cdots\cdots (12)$$

$$\hat{\mathbf{Y}} = \mathbf{C} \cdot \hat{\mathbf{X}} \quad \cdots\cdots\cdots (13)$$

Here,

$$\hat{\mathbf{X}} = [\hat{\omega}_p \ \ \hat{\omega}_s \ \ \hat{V}]^T, \ \mathbf{Y} = [\omega_p \ \ \omega_s]^T$$
$$\mathbf{U} = [\mathrm{Tin} \cdot \cos(11^\circ) \ \mathrm{Tout} \cdot \cos(11^\circ) \ \mu_{p0} F_p \ \ \mu_{s0} F_s]^T$$
$$\cdots\cdots\cdots (14)$$

The belt velocity is obtained from the 3rd term in state vector **X**. Matrices **A** and **B** have time varying coefficients. Matrix **K** is the observer gain, which is set so that the estimated value of the belt velocity coincides with the measured value on the bench. The estimated results are shown in **Fig. 18**, where the estimated values coincide with the measured values. Our finding, therefore, is that the slip velocity of the belt can be detected by using the estimation technologies described.

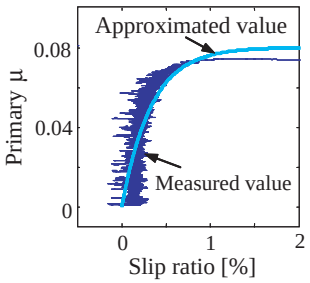

Fig. 17 Result of approximation of belt μ.

4. 3 Estimation of the belt friction margin

The experimental result of forcing a macro slip is shown in **Fig. 19**. Macro slip in the belt is caused by reducing the secondary clamping force. Belt μ_p and μ_s become large as the belt approaches the friction margin. The μ ratio, obtained by dividing μ_p by μ_s,

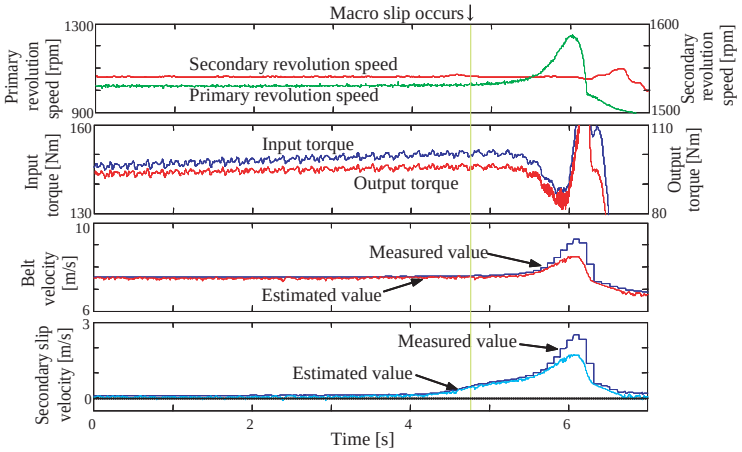

Fig. 18 Result of estimation of belt velocity and belt slip velocity (using bench data).

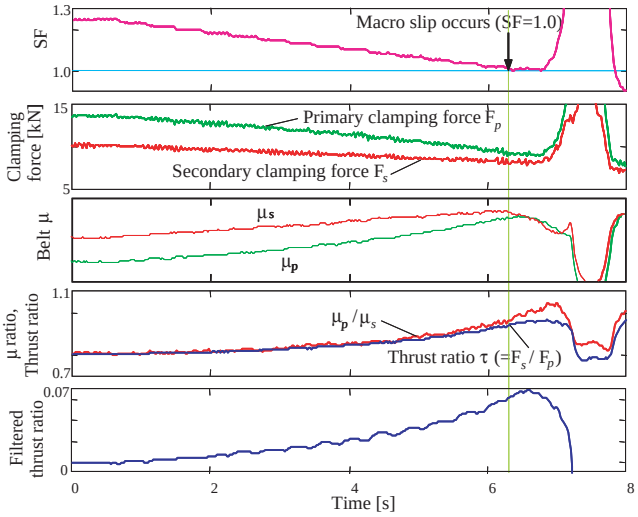

Fig. 19 Time chart of belt μ and μ ratio around macro slip occurrence.
(N_{in}=1000rpm, T_{in}=100Nm, speed ratio=1.0)

also becomes large because there is a difference of characteristic between belt μ_p and μ_s. The macro slip can be forecast by monitoring the increase of belt μ or the μ ratio. Belt μ monitoring cannot be used because belt μ is calculated using the torque measurement value. However, the μ ratio can be calculated as the ratio of the clamping force of both pulleys without torque. The μ ratio can be obtained from deformation of Eq. (1), as follows:

$$\frac{T_{out}}{T_{in}} = \frac{\eta \cdot T_{in} \cdot \gamma}{T_{in}} = \frac{2 \cdot \mu_s \cdot R_s \cdot F_s}{2 \cdot \mu_p \cdot R_p \cdot F_p} \quad \cdots\cdots\cdots (15)$$

Here, η is the torque transmitting efficiency, and its value is assumed to be 1.0. Using the relation $R_s = \gamma \cdot R_p$, Eq. (15) can be transformed as follows:

$$\mu_p / \mu_s \fallingdotseq F_s / F_p = \tau \quad \cdots\cdots\cdots\cdots (16)$$

The ratio of clamping forces is defined as thrust ratio τ. Thrust ratio τ coincides with the μ ratio until macro slip occurs. Thrust ratio τ is treated by a band-pass filter because its steady-state value changes due to the belt working condition. From **Fig. 19**, it can be determined by monitoring of the filtered value of the thrust ratio τ that the belt friction is at the end of the margin.

5. Conclusion

(1) We used a test apparatus consisting of a low inertia dynamo and various belt measurement technologies. The belt behavior in its actual working conditions has been clarified, and the data necessary for the analysis of power transmission characteristics have been obtained.

(2) The application of a state estimation technology has been examined for belt behavior, which is difficult to measure when a vehicle running. The result is that it is clear that the belt velocity and the friction margin of the belt can be estimated, and that the technology can be used as a tool for effective analysis in actual systems.

References

1) Yamaguchi, H., et al. : "Development of Belt Saturation Detection Method for V-Belt Type CVT", SAE Tech. Pap. Ser., No.2004-01-0479(2004)
2) Nishizawa, H., et al. : "Friction Characteristics Analysis for Clamping Force Setup in Metal V-Belt Type CVT", SAE Tech. Pap. Ser., No.2005-01-1462 (2005)
3) Kimura, M. : "An Ultra-small Sized Data-logger System for High-speed Rotation Measurement", Toyota Central R&D Rev., **40**-1(2005), 57 <http://www.tytlabs.co.jp/english/review/rev401epdf/e401_057kimura.pdf
4) Middleton, R. H. and Goodwin, G. C. : Digital Control and Estimation: A Unified Approach, (1990), Prentice Hall

(Report received on July 12, 2005)

Hiroyuki Yamaguchi
Research fields : Control and state estimation of power transmission system
Academic society : Jpn. Soc. Mech. Eng., Soc. Autom. Eng. Jpn.

Hirofumi Tani
Research fields : Dynamics analysis of power transmission system
Academic society : Jpn. Soc. Mech. Eng., Soc. Autom. Eng. Jpn.

Kisaburo Hayakawa
Research fields : Estimation, control, modeling and analysis of power transmission system
Academic degree : Dr. Eng.
Academic society : Soc. Instrum. Control Eng., Jpn. Soc. Mech. Eng., Soc. Autom. Eng. Jpn.